Published as: António B Mapossa, Walter W Focke, Alcides Sitoe, Homa Izadi, Elizbé du Toit, René Androsch, Chanita Sungkapreecha, L. van der Merwe. Mosquito repellent thermal stability, permeability and air volatility. *Pest Management Science,* 76**,** 1112-1120.

Mosquito repellent thermal stability, permeability and air volatility

António B Mapossa[1,2], Alcides Sitoe[1,2,3], Walter W Focke[1,2,*], Homa Izadi[1], Elizabeth L du Toit[1], René Androsch[4], Chanita Sungkapreecha[4], Elizabet M. van der Merwe[5]

[1]Institute of Applied Materials, Department of Chemical Engineering, University of Pretoria, Lynnwood Road, Pretoria, South Africa

[2]UP Institute for Sustainable Malaria Control & MRC Collaborating Centre for Malaria Research, University of Pretoria, Private Bag X20, Hatfield 0028, Pretoria, South Africa, Pretoria, South Africa

[3]Department of Chemistry, Eduardo Mondlane University, Maputo, Mozambique

[4]Interdisciplinary Center for Transfer-oriented Research in Natural Sciences, Martin Luther University Halle-Wittenberg, D-06099 Halle/Saale, Germany

[5]Department of Chemistry, University of Pretoria, Lynnwood Road, Pretoria, South Africa

Abstract

BACKGROUND: The effectiveness of mosquito repellents, whether applied topically on the skin or released from a wearable device, is crucially determined by the evaporation rate. This is because a repellent has to be present in the form of vapour in the vicinity of the exposed skin that needs protection. Therefore, gravimetric techniques were used to investigate the direct evaporation of selected liquid repellents, their permeation through polymer films, and their release from a microporous polyethylene matrix.
RESULTS: Evaporation of a repellent into quiescent air is determined by its air permeability. It is defined as the product of the vapour pressure and the diffusion coefficient, i.e. $S_A = P_A^{sat} D_A$. It was found that the repellent ranking, in terms of decreasing volatility, was ethyl anthranilate > citriodiol > dimethyl phthalate > DEET > decanoic acid > ethyl butylacetylaminopropionate > Icaridin. Experimental S_A values, at 50 °C, ranged from 0.015 ± 0.008 mPa·m^{2}s^{-1} for the least volatile repellent (Icaridin) up to 0.838 ± 0.077 mPa·m^{2}s^{-1} for the most volatile repellent (ethyl anthranilate). The release rate from microporous polyethylene strands, produced by extrusion-compounding into ice water baths followed a similar ranking. These strands featured an integral skin-like membrane that covered the extruded strands and controlled the release of the repellent at a low effective rate.
CONCLUSION: The high thermal and thermo-oxidative stability together with the low volatility of the mosquito repellents ethyl butylacetylaminopropionate and Icaridin make them attractive candidates for long-lasting wearable mosquito repellent devices. Such anklets/footlets/bracelets may have utility for outdoor protection against infective mosquito bites in malaria-endemic regions.

Keywords: Repellents; evaporation; diffusion coefficient; vapour pressure; permeability; polyethyelene

1. Introduction

Mosquito-borne diseases pose a serious health problem for people living in endemic regions, especially those in sub-Saharan Africa. Illnesses transmitted by mosquitoes include malaria, dengue fever, yellow fever as well as the Zika and chikungunya virus diseases. Millions of people are affected and many of them, especially children, die every year from mosquito-borne diseases [1, 2]. Topical applications of mosquito repellents can help minimize the risk of disease transmission and reduce the discomfort caused by mosquito bites [3, 4]. Most insect repellents act by producing a vapour barrier which prevents contact of the insect with the human skin [5, 6].

Repellent products include aerosol sprays, pump dispensers, lotions, creams, suntan oils, powders, grease sticks, and wearable devices [7]. The suitability and effectiveness of a repellent formulation depends on the nature of the repellent (e.g. active ingredient, formulation adjuvants) together with its inherent properties (vapour pressure, boiling point, odour, solubility) while environmental factors (temperature, humidity, wind) also affect performance. Compounds with too high vapour pressures tend to dissipate rapidly so that they soon fail to protect against mosquitos [3]. On the other hand, if the vapour pressure is too low, the concentration of the repellent in the air might be insufficient to be effective [8]. This means that the volatility is a very important physical property that affects the efficacy of a repellent.

Volatilisation (or vaporization) is a phase change process whereby a substance in a condensed phase is converted into a gaseous or vapour state. It occurs via processes such as sublimation (in case of a solid), evaporation, or boiling. Boiling is a bulk phenomenon while evaporation is a surface phenomenon, i.e. it occurs at the surface of the liquid. Evaporation happens at temperatures below the boiling temperature at a given pressure. In other words, it occurs when the partial pressure of vapour of the substance in the air environment is less than the equilibrium vapour pressure. As mentioned above, the volatilization behaviour is a crucial property that determines the efficacy of a topical mosquito repellent. A minimum effective

dose (MED) of the active ingredient close to the skin is required to repel the mosquitoes successfully [9]. Similarly, for space repellents, a minimum inhibitory concentration (MIC) of the repellent must be present in the bulk air [10]. The MED and MIC vary among repellents and they are functions of intrinsic repellence and environmental factors. Previous studies showed that the protection time was inversely proportional to the evaporation rate of the repellent [9, 11-13].

Ideally, the vapour concentration of the repellents should be controlled just above the minimum required level. This will provide effective protection for the longest possible time. If the vapour behaves like an ideal gas, the molar concentration in the ambient air is given by the expression [14]:

$$C_A = P_A^{sat} / RT \qquad (1)$$

where C_A and $P_A{}^{sat}$ are the concentration ($mol \cdot m^{-3}$) and the vapour pressure (Pa) of repellent *A*, respectively; *T* is the absolute temperature in K and R = 8.3145 $J \cdot mol^{-1}K^{-1}$ is the gas constant.

It can be shown that the vaporisation rate is directly proportional to the vapour pressure. This relationship is very general and arises from the assumptions of ideal gas behaviour, Raoult's law, and a negligible concentration of the sample compound far from the sample surface [15]. Equation (2) is the general form for the vaporisation rate at finite pressures [15]:

$$n_A = \left(\frac{M_A Sh}{L\,RT} \right) P_A^{sat} D_A \qquad (2)$$

where n_A is the mass flux of compound *A* ($kg \cdot m^{-2}s^{-1}$); M_A is the molar mass ($g \cdot mol^{-1}$); *L* is a characteristic length (m) of the sample geometry; D_A is the diffusion coefficient in (m^2s^{-1}), and *Sh* is the Sherwood number defined by k_cL/D_A with k_c the mass transfer coefficient ($m \cdot s^{-1}$).

Equation (2) can be applied to the evaporation of a liquid present in a partially filled cylindrical container [14, 16, 17]. This is conveniently studied with a thermogravimetric analysis (TGA) set-up. The sample geometry takes the form of a partially filled cylindrical sample cup with an inert purge gas sweeping over the top. For the situation where the rate of evaporation is controlled by diffusion through the stagnant gas layer present in the upper part of the cup, the rate of vaporisation is given by:

$$\frac{dm_A}{dt} = \left(\frac{M_A A}{zRT}\right) P_A^{sat} D_A \qquad (3)$$

where dm_A/dt is the TGA-measured rate of mass loss ($kg \cdot s^{-1}$); P_A^{sat} is the sample vapour pressure (Pa) at absolute temperature T (K); R is the gas constant (8.3145 $J \cdot mol^{-1}K^{-1}$); D_A is the diffusion coefficient (m^2s^{-1}) of the repellent in air; M_A is the molar mass ($g \cdot mol^{-1}$) of the vaporising compound, A is the cross-sectional surface area (m^2) of the cup, and z is the depth (m) of the gas filled part of the sample cup.

The primary objective of the present study was to generate data on repellents that will assist development of improved repellent products, specifically wearable devices in the form of bracelets or anklets. Towards this goal, gravimetric techniques were used to characterise thermal stability, vaporisation and polymer permeation properties for selected mosquito repellents. Oven ageing was used to establish thermal-oxidative stability at elevated temperatures. Gravimetric methods were employed to estimate and compare liquid repellent evaporation rates.

Polyethylene was chosen as the polymer matrix as the intended application is highly cost sensitive and also because it can be processed at lower temperatures than many other polymers. The permeability of blown polyethylene films were determined using Payne permeability cups. Repellent-filled microporous polyethylene strands were prepared by an extrusion process and the time-dependent release profiles were determined as a function of oven ageing time. The

intention was that the results generated should provide guidance for future commercial design and development of improved long-life repellent anklets and bracelets.

2. Materials and methods

2.1 Materials

Table 1 lists the suppliers and some of the physical properties of the solvent and the insect repellents considered in the present study. Dichloromethane was obtained from Merck and used for extractions. All compounds were used as received, i.e. without further purification. Linear low-density polyethylene (LLDPE) (grade HR411) was obtained from Sasol. The density was 0.939 g cm^{-3} and the MFI was 3.5 g/10 min (190 °C/2.16 kg). Dellite 43B organoclay was supplied by Laviosa Chimica Mineraria S.pA. The approximate median particle size was 8 μm. The clay was organo-modified with dimethyl benzyl hydrogenated tallow ammonium. It was used to modify the consistency of the liquid repellents. Pyrogenic nanosilica powder HDK N20 was obtained from Wacker Chemie. According to the manufacturer, the silica was amorphous and had a surface area of about 200 $m^2 \cdot g^{-1}$.

2.2 Extrusion compounding and film blowing

Polymer nanocomposites (without repellent) were prepared by dispersing the clay into the polymer powder with a Sigma spice grinder. The resulting powder blends were compounded on a TX28P 28 mm co-rotating twin-screw extruder with a screw diameter of 28 mm and an L/D ratio of 18. The screw design of this machine comprised intermeshing kneader blocks that also imparted a forward transport action. The extruded strands were cooled by passing them

Table 1. List of repellent chemicals, their properties and suppliers

Chemical	**CAS-Number**	**M/(g·mol^{-1})**	**ρ/(g·cm^{-3})**	**T_b /(°C)**	**T_m /(°C)**	**Purity/(%)**	**Supplier**
DEET	[CAS-No. 134-62-3]	191.27	0.998	288	-	97	Sigma-Aldrich
Ethyl anthranilate	[CAS-No. 87-25-2]	165.19	1.117	268	13-15	>96	Sigma-Aldrich
Dimethyl phthalate	[CAS-No. 131-11-3]	194.18	1.190	282	2	>99	Sigma-Aldrich
Decanoic acid	[CAS-No. 334-48-5]	172.26	0.893	268	27-32	>98	Sigma-Aldrich
Icaridin	[CAS-No. 119515-38-7]	229.30	0.98	296	#	>97	Saltigo
IR3535	[CAS-No. 52304-36-6]	215.29	0.998	292	#	>99	Merck-KGaA
Citriodiol®,*	[CAS-No. 1245629-80-4]	172.27	0.946	267	#	68	Citrefine International
Dichloromethane	[CAS No. 75-09-2]	84.93	1.33	40	-95	99	Merck-KGaA

* It is a mixture of components with isomers of *p*-menthane-3,8-diol as major constituents. # No information available

through a water bath. The strands were granulated on a Chen Shin Machinery Co., Ltd, Model CT-300 pelletizer and used to blow the films required for the permeability tests.

Strands containing the liquid repellents were produced in a similar manner except that they were not pelletized. Organoclay and/or pyrogenic silica nanofillers were included in all the formulations. This converted the liquid repellents into gel-like states which assisted the feeding of the mixture via the hopper of the compounding extruder. The nanofillers also facilitated good mixing and rapid dissolution of the repellent in the polymer melt. First, the polymer and organoclay powders were mixed in a container. Next, the required amount of liquid repellent was added slowly and mixed-in until a homogeneous semi-dry consistency was obtained that could be fed to the compounding extruder. The extrusion compounding was performed on the same TX28P 28 mm co-rotating twin-screw laboratory extruder. The temperature profiles, from hopper to die, was set at 140 /160 /160 /160 °C. The screw speed was 150 rpm. The exiting polymer strands were quench-cooled in an ice-water bath to ensure the formation of a co-continuous phase structure in the homogeneous polymer-repellent melt mixture exiting the extruder [18]. The rapid cooling induced phase separation via spinodal decomposition resulting in a co-continuous phase structure. In essence, a finely structured, open-cell foam-like polymer matrix is obtained with the liquid repellent trapped inside pores of micron-sized dimensions. The polyethylene strands, produced in this way, featured a membrane-like surface skin controlling the repellent release rate [18].

The films, used for permeability measurements, were blown using a Collin BL 180/400 blown film unit. It comprised a 30 mm diameter single screw extruder with L/D = 25. The blown film die had a diameter of 60 mm and featured a dual-lip cooling ring. The extruder was operated at a screw speed of 40 rpm. The temperature profiles, from hopper to die, were 170/190/190/190/190/190/190/190 °C.

The diameters of polymers strands were measured with a Mitutoyo Digital Calliper with a measurement range up to 150 mm. LLDPE strands with diameters ranging from 2.2 to 5.1 mm were obtained. The reported diameters of LLDPE strands represent the average of fifteen separate measurements along each strand. The final film thicknesses were measured with a Mitutoyo Digital micrometer with a resolution of 1 μm. The reported film thicknesses represent the average of five separate measurements.

2.3 Film permeability

The permeability of blown films was determined using aluminium Payne permeability cups. The internal diameter of the cups was 54.9 mm and they had a depth of 19.7 mm. They were partially filled with mosquito repellent before clamping the polymer films in place. The cups were placed in convection ovens set at a temperature of 50 ºC. The mass loss was measured daily over a period of two weeks. The permeability was estimated from the slope of the linear portion of the mass loss vs. time plot. Reported values represent the averages of duplicate determinations and the indicated uncertainties correspond to one standard deviation. Open cups, placed in the convection ovens, were also used to measure the evaporation rate at 50 °C.

2.4 Thermal-oxidative stability

Fourier transform infrared (FTIR) spectra of repellent samples were recorded on a Perkin-Elmer Spectrum 100 fitted with the universal attenuated total reflection (ATR) sampling accessory. The FTIR spectra were recorded in absorbance units in the wavenumber range from 4000 to 600 cm^{-1} at a resolution of 4 cm^{-1}. The reported spectra represent averages of 16 scans.

During the extrusion of the strands, the mosquito repellents were exposed to typical polymer processing temperatures, i.e. >180°C. It was deemed necessary to determine whether the repellents could withstand short time exposure to such high temperatures. Therefore, the heat stability was evaluated using the following procedure: Approximately 6 g repellent was placed in an open Polytop glass vial and exposed to high heat in either an EcoTherm-Labcon or a Scientific Series 9000 forced convection oven. The exposure was to a temperature of 200 °C for 30 min or to 50 °C for four months. FTIR spectra of the neat and exposed samples were compared to assess whether significant thermal-oxidative degradation had occurred.

2.5 Repellent content by solvent extraction

Approximately 70 mm lengths of the repellent-containing polymer strands were cut, weighed and placed in Polytop glass vials. About 40 mL dichloromethane was added before the vials were stoppered. The extraction solvent was replaced on a daily basis. After the fifth extraction, the strands were removed and allowed to dry in a fume hood at ambient temperature. The repellent content was estimated from the recorded mass loss of the strands. Reported results represent the average of triplicate evaluations.

2.6 Thermogravimetric analysis

The TGA instruments, diameters, pan dimensions and the conditions used to estimate evaporation of repellents are listed in Table 2. Duplicate evaluations on several different instruments were used in order to check the reproducibility of dynamic volatilisation data collection. Samples, weighing approximately 16 mg, were heated from ambient temperature up to 300 °C at a rate of 10 $K \cdot min^{-1}$. The purge gas was N_2 flowing at 100 $mL \cdot min^{-1}$.

T**able 2.** The TGA instruments, and the depth and internal diameter of the pans, used to determine the evaporation rate of repellents

TGA Instrument	**Mettler Toledo SDTA851**	**TA Instrument Q600**	**Convection oven**
Pan material	Alumina	Alumina	Aluminium
D_{pan}/(mm)	5.16	6.2	54.91
H_{pan}/(mm)	4.56	3.64	19.71
Temperature scan range/(°C)	30 - 300	50 -150	50
N_2 flow rate/(mL·min^{-1})	100	100	-

Table 3. Permeation of repellents through a neat polyethylene film and a nanocomposite film containing 5 wt-% Dellite 43B clay. The permeability was measured at 50°C and it is stated in units of g·µm·day^{-1}·m^{-2}

Repellent/Polymer film	**Neat LLDPE**	**LLDPE-43B**
DEET	289 ± 32	304 ± 35
Icaridin	126 ± 4	104 ± 3
IR3535	140 ± 32	129 ± 25
Ethyl anthranilate	1369 ± 31	2176 ± 31

2.7 Repellent release from polymer strands

The time-dependent release of the repellents from the strands was determined by ageing at 50 °C in either a Scientific Series 9000 or an EcoTherm-Labcon forced convection oven. The strands were suspended from the inside roof of the ovens in the form of loose coils and they were weighed twice a week. The mass loss and repellence testing were done for at least 45 days and in some cases for up to 120 days.

2.8 Correlating and predicting vapour pressures and air diffusion coefficients

Vapour pressure data for the repellents was gleaned from a variety of literature sources. Experimental data were correlated using established vapour pressure equations, i.e. Antoine, Wagner [19], and Cox [20, 21]. Where insufficient data was available, the vapour pressure curve was predicted using the method proposed by Myrdal and Yalkowsky [22]. The diffusion coefficients, for the repellent in air, were estimated using the procedure proposed by Wilke and Lee [23] and implemented according to the descriptions given in Poling, Prausnitz, John Paul and Reid [19]. The predicted repellent air permeability ($S_A = P_A^{sat} D_A$) values were subsequently determined from the product of the vapour pressure and the diffusion coefficient evaluated at the temperature of interest. Details of these procedures are provided in the Supplementary Material.

3 Results and discussion

3.1 Thermo-oxidative stability of repellents

FTIR spectra for the repellents in neat form and after thermal-oxidative stability testing by exposure to air for either 4 months at 50 °C or 30 min at 200 °C are presented in Figure S-1 in the Supplementary Material. Spectra for ethyl butylacetylaminopropionate are shown in Figure

1. The infrared absorption bands for the repellents were not affected by short-term heat exposure at 200 °C. This was also the case for most repellents after long term exposure to air at 50 °C. The exceptions were dimethylphthalate and ethyl butyl acetylaminopropionate. For these two repellents new carbonyl bands developed at ca. 1690 cm^{-1} and 1685 cm^{-1}, respectively. However, these new peaks were very small compared to the carbonyl absorption bands of the neat parent molecules. This is illustrated in the FTIR spectra for ethyl butylacetylaminopropionate shown in Figure 1. The indications are that oxidative degradation had commenced when these two repellents were exposed to warm air at 50 °C for four months. The apparently lower thermal-oxidative stability of ethyl butylacetylaminopropionate, compared to the other repellents, is tentatively attributed to its higher aliphatic character. Despite these observations, it can be concluded that the repellents investigated were able to withstand typical polymer processing temperatures for short periods of time. The fact that they also stayed essentially intact for several months at 50 °C suggests that they may retain repellent activity for comparable lengths of time.

3.2 Repellent evaporation

Figure 2 compares predicted temperature dependences of the air permeability of the repellents to values extracted from experimental thermogravimetric evaporation rate data. The experimental data are in reasonable agreement with predictions at elevated temperatures. However, significant discrepancies are apparent at lower temperatures, especially for DEET and ethyl anthranilate. In most cases the predicted curves fall well below the measurements. Interestingly, the Payne cup evaporation results agreed more closely with the TGA results than the theoretical predictions.

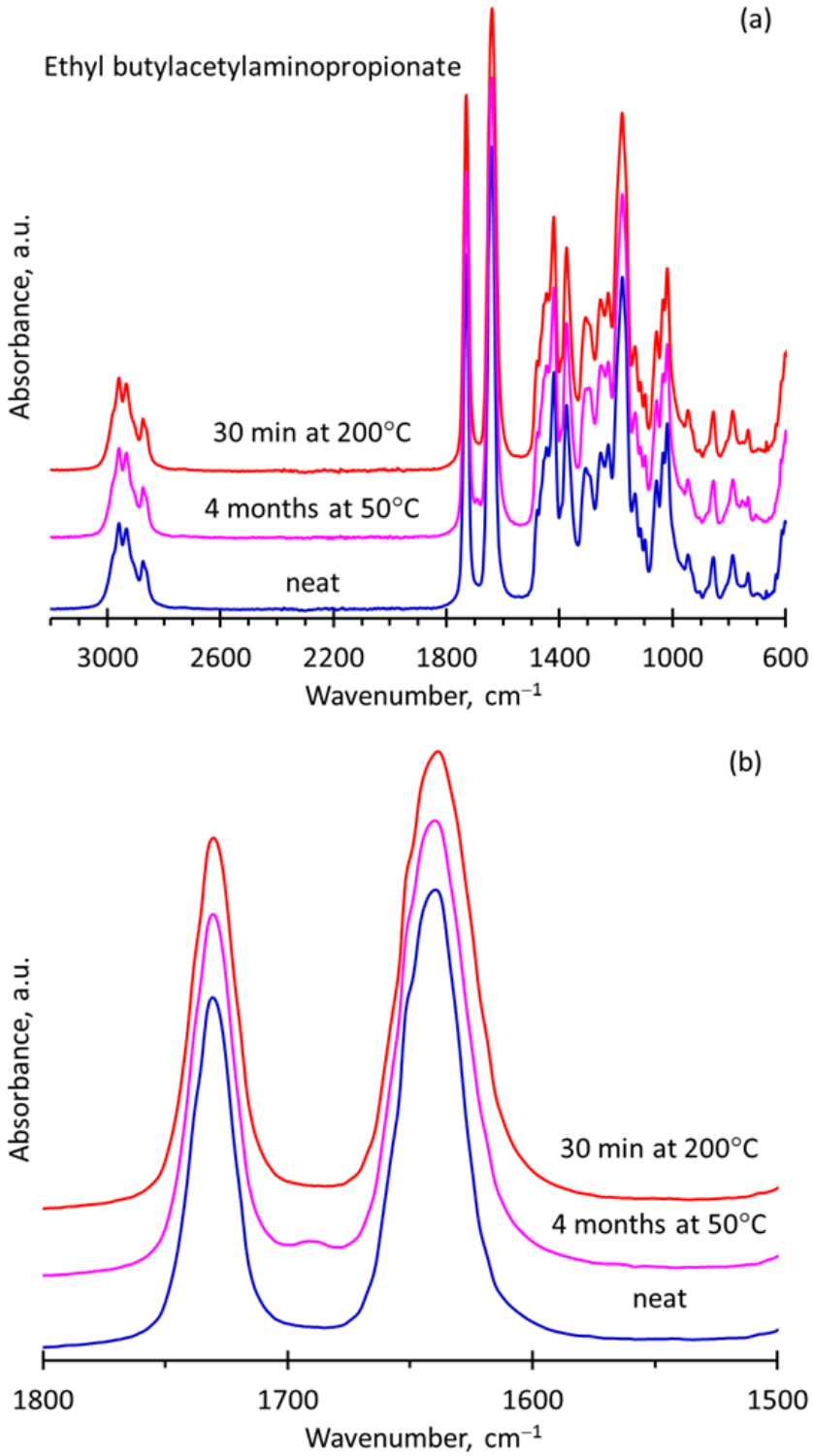

Figure 1. (a) FTIR spectra for the mosquito repellent ethyl butylacetylaminopropionate before and after thermal-oxidative stability testing by exposure to air at either 50 °C for four months or for 30 min at 200 °C. (b) Expanded view of the carbonyl absorption region showing the development of a new band near 1690 cm^{-1}.

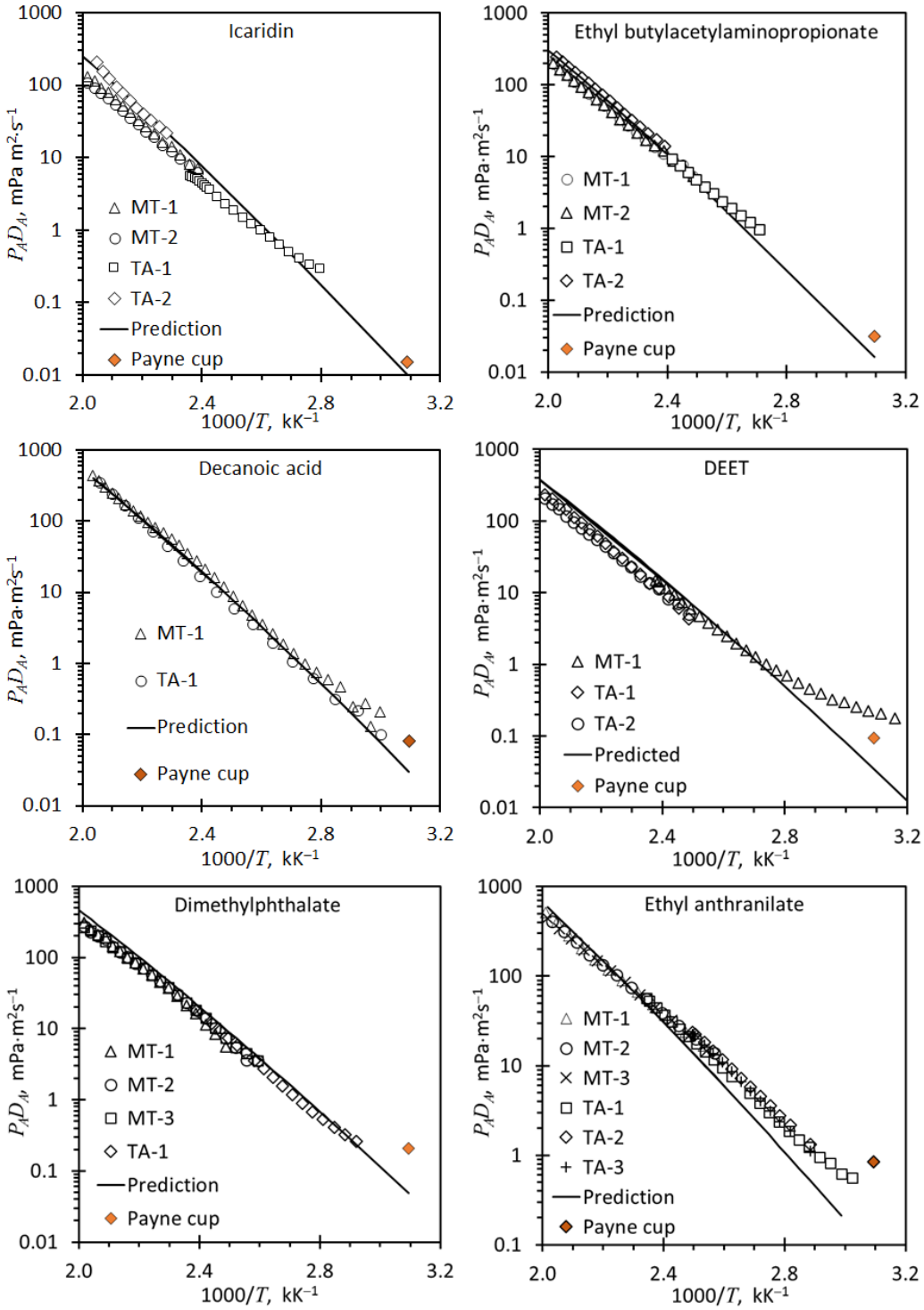

Figure 2. Comparison of air permeabilities, experimentally determined (symbols) and theoretically predicted (solid line), for Icaridin, ethyl butylacetylaminopropionate, decanoic acid, DEET, dimethyl phthalate and ethyl anthranilate. The replicate repellent evaporation runs were performed on Mettler Toledo SDTA851 (MT) and TA Instruments Q600 (TA) instruments.

Figure 3 shows the air permeabilities of the repellents determined with Payne cups at 50 °C. The $S_A = P_A^{sat} D_A$ values span more than one order of magnitude: Both ethyl anthranilate and citriodiol are fifty times more volatile than Icaridin. The volatility sequence at 50 °C, i.e. near-ambient conditions, was as follows: ethyl anthranilate > citriodiol > dimethyl phthalate > DEET > decanoic acid > ethyl butylacetylaminopropionate > Icaridin. Since Icaridin, ethyl butylacetylaminopropionate and DEET had the lowest evaporation rates, it is likely that they would be able to provide longer protection times against mosquitoes. In contrast, ethyl anthranilate and citriodiol showed higher evaporation rates, which may imply a shorter potential protection time depending on the concentration required for effective repellence. These conjectures were confirmed by actual repellence test results obtained for repellent-containing polyolefin strands [18].

3.3 Permeability of polyethylene films

Table 3 lists the permeability of the neat polymer and polymer-clay nanocomposite films to the repellents. The permeability ranking in the films was ethyl anthranilate > DEET > ethyl butylacetylaminopropionate > Icaridin. Noteworthy is the observation that the permeability of the nanocomposite film, to a given repellent, did not differ appreciably from that of the neat polyethylene film. This was confirmed by performing a t-test which showed that the difference between the two means was not statistically significant. This behaviour is in contradiction to the conventional wisdom with respect to sheet-like nanocomposites. It was expected that the

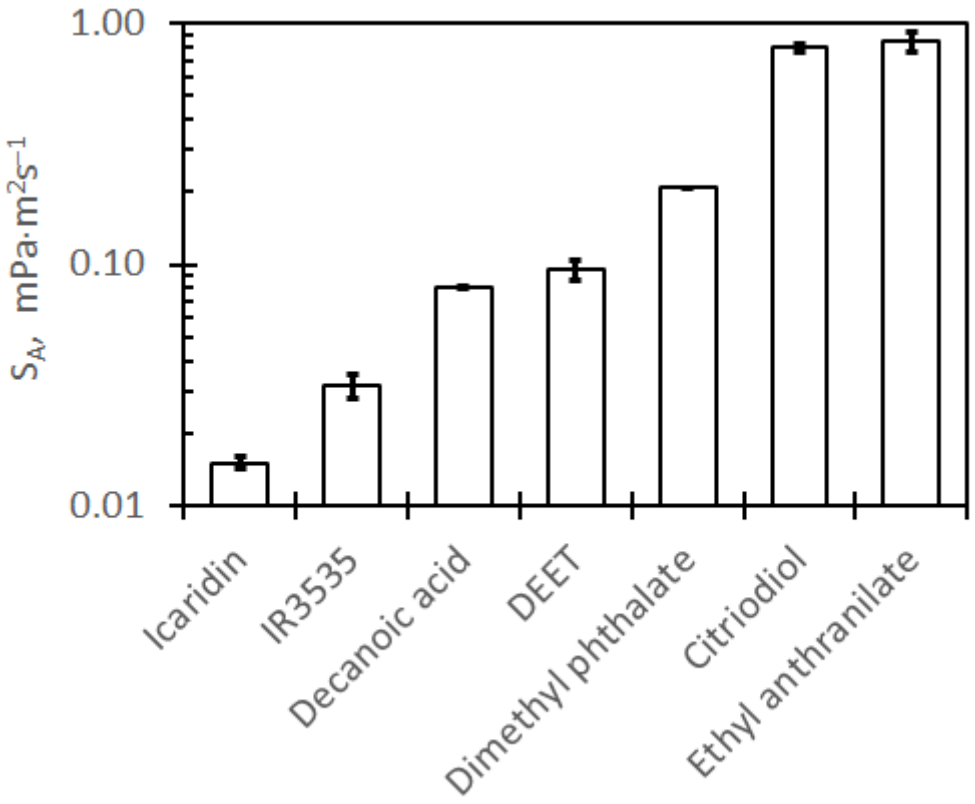

Figure 3. Air permeabilities of the repellents Icaridin, ethyl butylacetylaminopropionate, decanoic acid, DEET, dimethyl phthalate, citriodiol and ethyl anthranilate measured at 50 °C using Payne cups.

impermeable clay platelets, if properly exfoliated and dispersed in the matrix, would decrease the permeability because of a tortuous diffusion path effect. It is speculated that the observed opposite result could be attributed to poor matrix-filler adhesion which resulted in the formation of a porous microstructure that increased the mobility of the volatile repellents through the polymer film. Manninen et al. [24] showed that the processing path taken to prepare the nanocomposites may result in agglomeration of the layers of the organoclay. According to Choudalakis et al. [25], aggregation of the silicate layers leads to a reduction of the aspect ratio and that affects the permeation properties of the nanocomposite. Furthermore, such agglomerates may form large-scale pores in the matrix, which can act as low-resistance pathways for vapour transport within the nanocomposite [25]. Another, speculative possibility is that the polar surfactant phase associated with the organoclay assisted the dissolution and diffusion of the repellents in the polyethylene matrix. In summary, the present study demonstrated that the incorporation of the Dellite 43B organoclay did not lead to the expected lowering of film permeability. This means that the nanofillers' purpose was limited to that of providing the necessary processing aid functionality.

3.4 Repellent evaporation from extruded strands

Table 4 lists the composition and dimensions of the polyethylene strands used for repellent release studies. Figure 4 to Figure 8 show repellent release curves for polyethylene strands aged at 50 ^{o}C in a convection oven. The solid lines shown in these Figures correspond to least square data fits to the implicit theoretical expression that links the amount of repellent released from a microporous cylindrical body with a membrane coating (X) to the elapsed time (t) [18]:

$$\kappa_1 t = \kappa_2 \left(1 - X\right) + X \ell n X \qquad (4)$$

Table 4. Composition and dimensions of the polyethylene strands used for repellent release studies. All strands contained 5 wt-% clay

Repellent	Repellent content wt-%	Strand diameter mm	Equation (4) parameters κ_1	κ_2	Initial evaporation rate (dX/dt) (day^{-1})	Membrane thickness (μm)
DEET	20.2 ± 0.5	3.42 ± 0.16	0.00295	1.137	0.0215	17
DEET	19.3 ± 0.6	4.39 ± 0.17	0.00206	1.308	0.00668	44
DEET	20.2 ± 0.5	4.61 ± 0.17	0.00185	1.049	0.0376	7.0
DEET	29.3 ± 0.9	2.87 ± 0.15	0.00205	1.087	0.0235	19
DEET	30.0 ± 0.8	4.08 ± 0.12	0.00394	2.317	0.00299	104
DEET	29.3 ± 0.9	4.66 ± 0.21	0.00146	1.079	0.0185	15
Icaridin	19.7 ± 0.6	2.26 ± 0.05	0.00143	1.168	0.00850	26
Icaridin	18.5 ± 0.8	2.89 ± 0.10	0.00157	1.112	0.0141	12
Icaridin	20.2 ± 0.5	3.84 ± 0.18	0.1640	175.0	0.000944	139
Icaridin	19.7 ± 0.6	4.54 ± 0.23	0.000545	1.080	0.00680	16
Icaridin	31.0 ± 0.6	2.15 ± 0.06	0.000657	1.129	0.00509	46
Icaridin	29.5 ± 0.8	2.60 ± 0.09	0.00121	1.128	0.00949	20
Icaridin	29.0 ± 0.2	3.96 ± 0.17	0.269	397.5	0.000678	186
Icaridin	31.0 ± 0.6	4.63 ± 0.25	0.000351	1.055	0.00639	17
DEET	27.7 ± 0.2	3.17 ± 0.41	0.00889	1.906	0.00981	41
Icaridin	27.4 ± 0.3	3.74 ± 0.31	0.3050	337.9	0.000906	148
Ethyl anthranilate	26.6 ± 0.2	3.63 ± 0.73	0.0110	1.000	-	-
IR3535	25.5 ± 0.2	3.59 ± 0.39	0.8470	494.9	0.00171	88

Where t is the time, and κ_1 and κ_2 are parameters that depend on the strand structure and dimensions, the compositions as well as temperature dependent physical properties. They are constants for a given fixed strand size, formulation and test temperature. The two constants embody the main factors determining the release rate: (i) The effect of differences in the membrane thickness of the strands; and (ii) the relative vapour pressures of the repellents. Previous studies showed that the thickness of the membrane that covers the strands had a dominant effect on the rate of repellent release [18].

Figure 4 shows the effect of the nature of the repellent (ethyl anthranilate, DEET, ethyl butylacetylaminopropionate and Icaridin) on compounded and extruded strands containing 5 wt-% organoclay 43B and 30 wt-% repellent. Ethyl anthranilate was released at the highest rate and Icaridin at the lowest rate from the strands, in accordance with their respective volatilities. Similar results (not shown) were obtained with pyrogenic silica as nanofiller and repellents loaded at 40 wt-%. In that case the ethyl anthranilate-based strand was practically exhausted within the first 40 days of exposure. However, the other repellents were released at a nearly constant rate over a longer time period. The solid lines in Figure 4 show that equation (4) provided reasonable fits to the experimental data.

Figure 5 shows the effect of the nature of the nanofiller on the time-dependent release of DEET during oven ageing at 50 °C. The LLDPE strands contained 5 wt-% organoclay and/or pyrogenic silica. The sample that contained both fillers showed the fastest release of DEET while it was slowest with the clay as filler. It is not clear what the reason for this is but it does suggest that the incorporation of organoclay could provide for longer release time. Similar behaviour was observed with Icaridin as repellent.

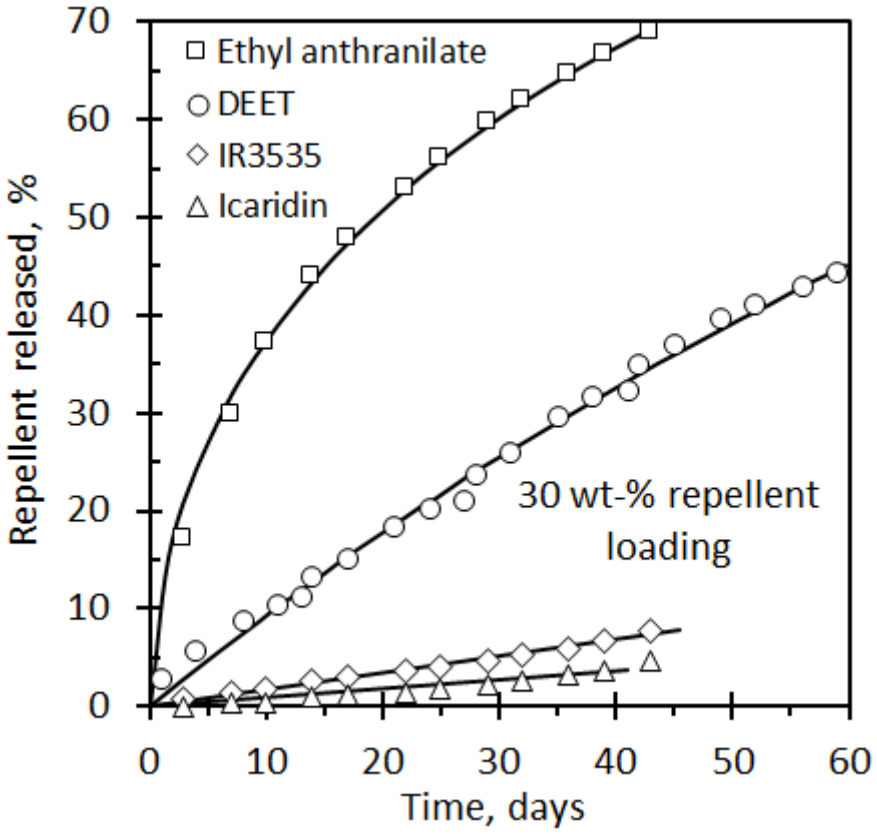

Figure 4. Effect of the nature of the repellent on the release from LLDPE strands during oven ageing at 50°C. The LLDPE strands contained 5 wt-% organoclay 43B and 30 wt-% repellent.

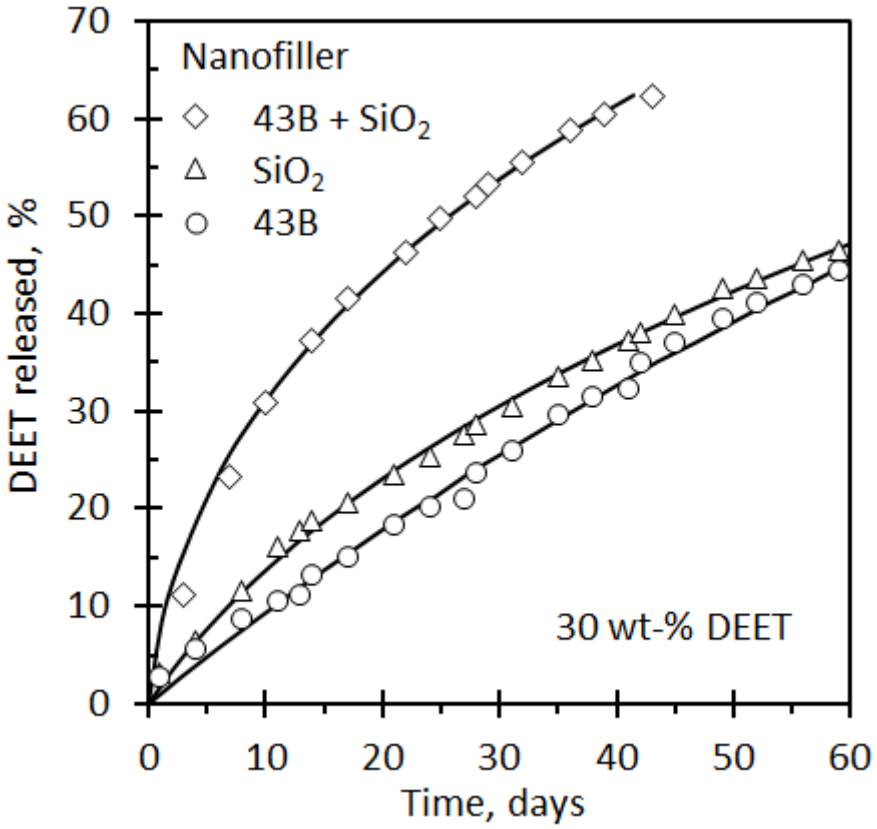

Figure 5. The effect of the nature of the nanofiller on the release of DEET from LLDPE strands aged at 50°C. The LLDPE strands contained 30 wt-% DEET and 5 wt-% fumed silica and/or organoclay.

Figure 6 shows the effect of organoclay loading on the time-dependent release of Icaridin from LLDPE strands aged at 50 °C. Interestingly, the release rate increased as the clay content was increased. This was unexpected as the clay platelets are known to be impermeable to the repellents. However, this observation accords with the observations that the permeability of the blown films also increased when clay was incorporated. Figure 7 shows that the relative release rate also increases as the repellent loading, in this case for DEET, is increased. Figure 8 shows the effect of strand diameter on the release of Icaridin loaded at 30 wt-% with the organoclay set at 5 wt%. There is no discernible trend for release rate as a function of strand diameter. This is attributable to the differences in the thickness of the membrane covering the strands, a factor that was unfortunately not controllable in the present study.

3.10 Estimation of the membrane thickness

At the commencement of the repellent release experiment, it can be assumed that the microporous inner part of the strands is completely filled with repellent [18]. The initial flux or repellent, at this point in time, is completely determined by the permeability of the membrane coating, if present. According to equation (4) this flux amounts to

$$-\frac{dX}{dt} = \frac{\kappa_1}{\kappa_2 - 1} \qquad (5)$$

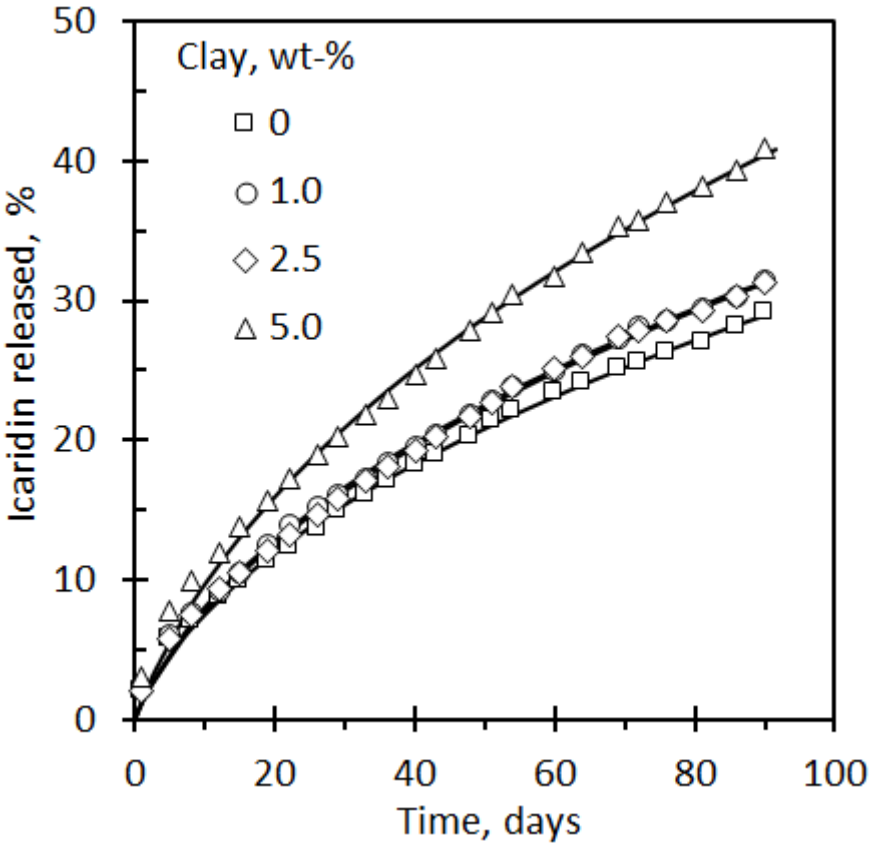

Figure 6. The effect of clay content on the release of Icaridin from LLDPE strands aged at 50 °C. The strands contained 20 wt-% repellent.

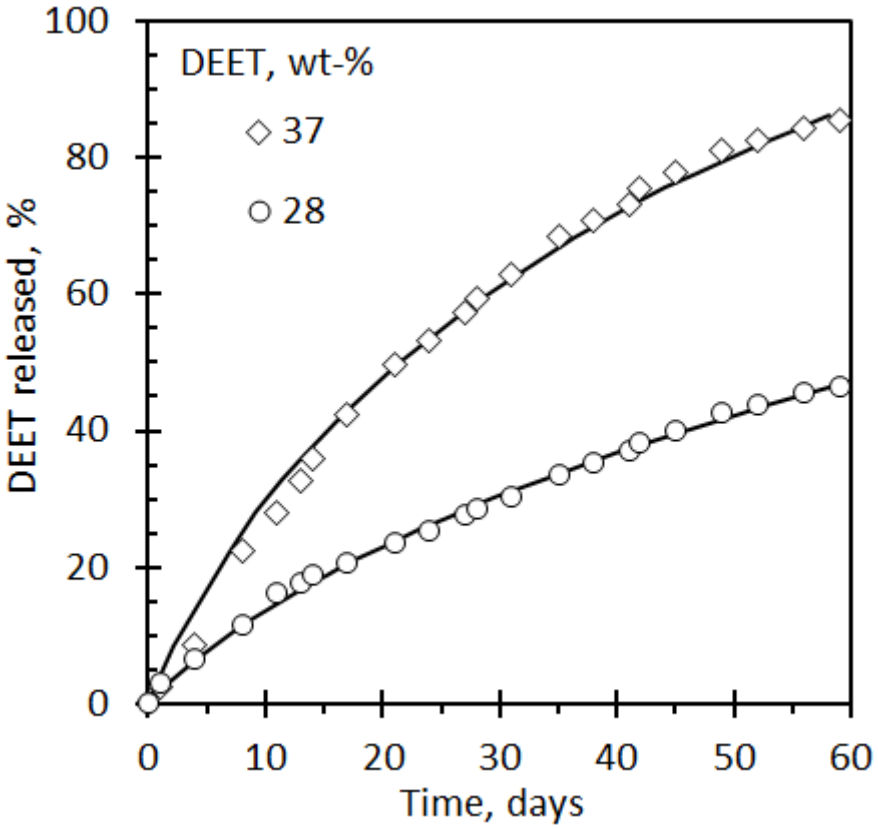

Figure 7. Effect of repellent loading on the release of DEET from LLDPE strands, filled with 5 wt-% fumed silica, during oven ageing at 50°C.

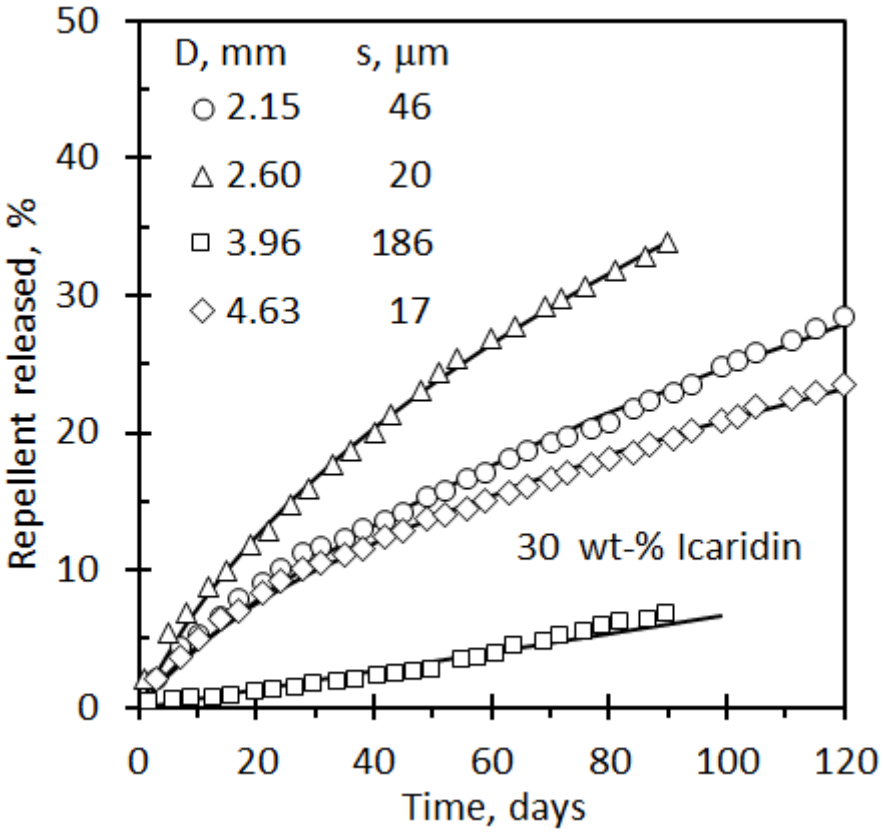

Figure 8. The effect of strand diameter (*D*) on the release of Icaridin from LLDPE strands during oven ageing at 50 °C. The strands contained 5 wt-% organoclay 43B and 30 wt-% repellent. The lack of a discernible trend with strand diameter is attributed to the different thickness values (*s*) of the covering membranes.

Equation (5) shows that the flux can be estimated from the data fit parameters of equation (4) to the experimental data. The thickness of the strand membrane (*s*) is defined by the expression:

$$s = -\pi DLP \Big/ \left(m \frac{dX}{dt} \right) \qquad (6)$$

where *s* is the membrane thickness in μm; *D* and *L* are the diameter and length of the strand in m respectively; *m* is mass of repellent initially present in g; *P* is the permeability of the membrane which is assumed to be the same as the value measured for the blown film containing the organoclay listed in Table 3.

The values of the thickness of the skin-like membranes covering the strands were estimated from the repellent release data in combination with the permeability values measured for the films. The calculated membrane thicknesses varied from effectively zero for a strand containing ethyl anthranilate, to 186 μm for a strand containing Icaridin. The SEM image of the latter strand is shown in Figure 9 and it revealed that the strands did indeed feature a thin dense skin on the surface of approximately the same thickness as estimated from the repellent release rate.

4 Conclusions

The evaporation into air, and the permeability through polyethylene films, of selected commercial mosquito repellents was evaluated. The evaporation into quiescent air is determined by the air permeability, defined as the product of the vapour pressure and the diffusion coefficient, i.e. $S_A = P_A^{sat} D_A$. The repellent ranking in terms of decreasing volatility was: ethyl anthranilate > citriodiol > dimethyl phthalate > DEET > decanoic acid > ethyl butylacetylaminopropionate > Icaridin. At 50 °C, experimental S_A values ranged from 0.015 ±

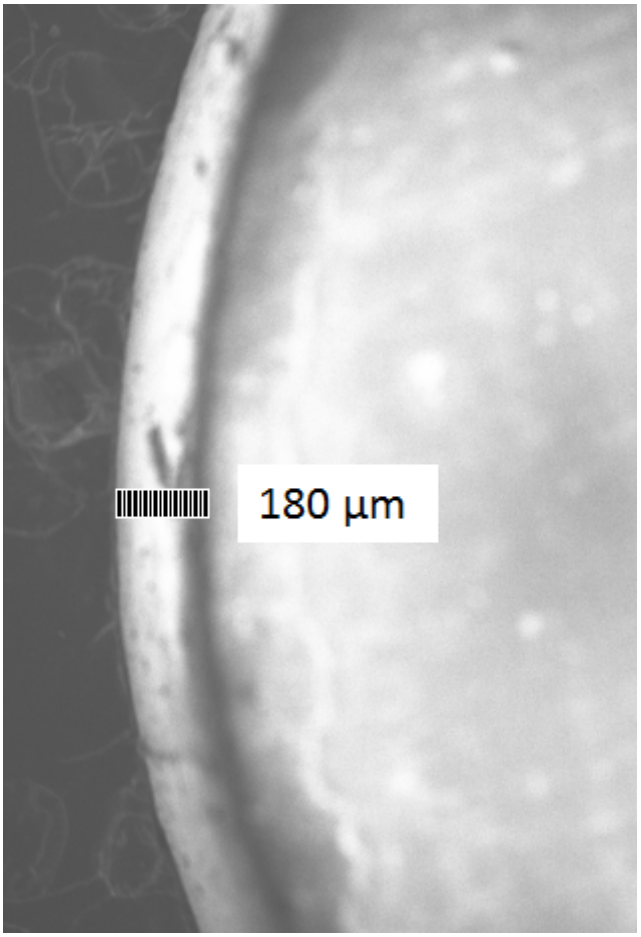

Figure 9. Scanning electron microscope (SEM) micrograph showing the cross-section of a polyethylene strand containing 29 wt-% Icaridin and 5 wt-% clay 43B. The integral surface skin is clearly visible and it is about 180 µm thick.

0.008 mPa·m^{2}s^{-1} for the least volatile repellent (Icaridin) to 0.838 ± 0.077 mPa·m^{2}s^{-1} for the most volatile repellent (ethyl anthranilate). The permeation rates of the repellents through a neat polyethylene film and a nanocomposite film containing 5 wt-% Dellite 43B clay did not differ appreciably. Values measured at 50 °C followed a ranking similar to the one observed for the air permeability. Experimental values obtained for nanocomposite films ranged from 119 ± 3 g·μm·day^{-1}·m^{-2} for the least volatile repellent (Icaridin) to 2176 ± 31 g·μm·day^{-1}·m^{-2} for the most volatile repellent (ethyl anthranilate). Polyethylene strands, filled with high levels of repellents, were obtained by an extrusion-compounding process. The internal structure took the form of an open-cell foam. This was covered by a thin integral skin. The thickness of this membrane essentially controlled the release of the liquid repellent trapped inside the microporous internal structure of the strands. Repellent depletion took more than a few months for strands aged at 50 °C in convection ovens. These results suggest the possibility of developing long-life wearable mosquito repellent devices. Such anklets/footlets/bracelets may have utility for outdoor protection against infective mosquito bites in malaria-endemic regions.

Acknowledgements

This work was funded by the Deutsche Forschungsgemeinschaft (DFG) (Grant AN 212/22-1). Saltigo (Germany) is thanked for the generous gift of Saltidin samples and Laviosa Chimica Mineraria S.p.A (Italy) for providing the Dellite 43B organoclay sample. We also express our gratitude to Dr Gimo Daniel and Mr Robert Tewo for reviewing the manuscript and Dr Isbé van der Westhuizen for assistance with thermogravimetric analysis.

References

1. Fasulo TR, History and insects. *Encyclopedia of Entomology*: 1810-1826 DOI Electronic Resource Number (2008).

2. WHO. World Malaria Report 2015, ed. by WHO. World Health Organisation: Switzerland (2015).
3. Islam J, Zaman K, Duarah S, Raju PS and Chattopadhyay P, Mosquito repellents: An insight into the chronological perspectives and novel discoveries. *Acta Tropica*; **167**(216-230 DOI Electronic Resource Number (2017).
4. Diaz JH, Chemical and plant-based insect repellents: efficacy, safety, and toxicity. *Wilderness & environmental medicine*; **27**(1): 153-163 DOI Electronic Resource Number (2016).
5. Nogueira Barradas T, Perdiz Senna J, Ricci Junior E and Regina Elias Mansur C, Polymer-based Drug Delivery Systems Applied to Insects Repellents Devices: A Review. *Current drug delivery*; **13**(2): 221-235 DOI Electronic Resource Number (2016).
6. Nerio LS, Olivero-Verbel J and Stashenko E, Repellent activity of essential oils: a review. *Bioresource technology*; **101**(1): 372-378 DOI Electronic Resource Number (2010).
7. Rodriguez SD, Chung H-N, Gonzales KK, Vulcan J, Li Y, Ahumada JA, Romero HM, De La Torre M, Shu F and Hansen IA, Efficacy of Some Wearable Devices Compared with Spray-On Insect Repellents for the Yellow Fever Mosquito, Aedes aegypti (L.) (Diptera: Culicidae). *Journal of insect science (Online)*; **17**(1): 24 DOI Electronic Resource Number (2017).
8. Brown M and Hebert AA, Insect repellents: an overview. *Journal of the American Academy of Dermatology*; **36**(2): 243-249 DOI Electronic Resource Number (1997).
9. Maibach HI, Khan AA and Akers W, Use of insect repellents for maximum efficacy. *Archives of Dermatology*; **109**(1): 32-35 DOI Electronic Resource Number (1974).
10. Ariëns EJ. *Drug Design: Medicinal Chemistry: A Series of Monographs*. Elsevier, (2016).
11. Kasman S, EOADHOUSE L and Wright G, Studies in Testing Insect Repellents. *Mosquito News*; **13**(2): 116-123 DOI Electronic Resource Number (1953).
12. Smith CN. *Factors affecting the protection period of mosquito repellents*. US Dept. of Agriculture, (1963).
13. Gabel M, Spencer T and Akers W, Evaporation rates and protection times of mosquito repellents. *Mosquito News* 1976).
14. Pieterse N and Focke WW, Diffusion-controlled evaporation through a stagnant gas: Estimating low vapour pressures from thermogravimetric data. *Thermochimica Acta*; **406**(1-2): 191-198 DOI Electronic Resource Number (2003).
15. Focke WW, A revised equation for estimating the vapour pressure of low-volatility substances from isothermal TG data. *Journal of Thermal Analysis and Calorimetry*; **74**(1): 97-107 DOI Electronic Resource Number (2003).
16. Parker A and Babas R, Thermogravimetric measurement of evaporation: Data analysis based on the Stefan tube. *Thermochimica Acta*; **595**(67-73 DOI Electronic Resource Number (2014).
17. Rong Y, Gregson CM and Parker A, Thermogravimetric measurements of liquid vapor pressure. *Journal of Chemical Thermodynamics*; **51**(25-30 DOI Electronic Resource Number (2012).
18. Mapossa AB, Sibanda MM, Sitoe A, Focke WW, Braack L, Ndonyane C, Mouatcho J, Smart J, Muaimbo H, Androsch R and Loots MT, Microporous polyolefin strands as controlled-release devices for mosquito repellents. *Chemical Engineering Journal*; **360**(435-444 DOI Electronic Resource Number (2019).
19. Poling BE, Prausnitz JM, John Paul OC and Reid RC. *The properties of gases and liquids*. Mcgraw-hill New York, (2001).

20. Roháč V, Musgrove JE, Ružička K, Ružička V, Zábranský M and Aim K, Thermodynamic properties of dimethyl phthalate along the (vapour+ liquid) saturation curve. *The Journal of Chemical Thermodynamics*; **31**(8): 971-986 DOI Electronic Resource Number (1999).
21. Gobble C, Chickos J and Verevkin SP, Vapor pressures and vaporization enthalpies of a series of dialkyl phthalates by correlation gas chromatography. *Journal of Chemical & Engineering Data*; **59**(4): 1353-1365 DOI Electronic Resource Number (2014).
22. Myrdal PB and Yalkowsky SH, Estimating pure component vapor pressures of complex organic molecules. *Industrial & Engineering Chemistry Research*; **36**(6): 2494-2499 DOI Electronic Resource Number (1997).
23. Wilke C and Lee C, Estimation of diffusion coefficients for gases and vapors. *Industrial & Engineering Chemistry*; **47**(6): 1253-1257 DOI Electronic Resource Number (1955).
24. Manninen AR, Naguib HE, Nawaby AV and Day M, CO2 sorption and diffusion in polymethyl methacrylate–clay nanocomposites. *Polymer Engineering & Science*; **45**(7): 904-914 DOI Electronic Resource Number (2005).
25. Choudalakis G and Gotsis A, Permeability of polymer/clay nanocomposites: a review. *European Polymer Journal*; **45**(4): 967-984 DOI Electronic Resource Number (2009).